16,03

Near-surface excitation of the non-steady-state photo-EMF in a $PbNi_{1/3}Nb_{2/3}O_3$ crystal

© M.A. Bryushinin, I.A. Sokolov

Ioffe Institute,
St. Petersburg, Russia

E-mail: mb@mail.ioffe.ru

Received September 27, 2023
Revised September 27, 2023
Accepted November 30, 2023

The relaxor ferroelectric $PbNi_{1/3}Nb_{2/3}O_3$ is studied by the non-steady-state photo-EMF technique at wavelength $\lambda = 457$ nm corresponding to the light absorption edge of the crystal. This enables both the near-surface recording of diffusion charge gratings and photo-EMF signal excitation. The signal amplitude depends on the frequency of phase modulation of light, intensity and spatial frequency of the interference pattern. Analyzing these dependencies, we estimate the photoelectric parameters of the crystal — the type, value and relaxation time of photoconductivity, as well as the diffusion length of charge carriers.

Keywords: non-steady-state photo-EMF, photoconductivity, relaxor ferroelectric.

DOI: 10.21883/0000000000

1. Introduction

For relaxor perovskite ferroelectric (relaxors) materials, including $PbNi_{1/3}Nb_{2/3}O_3$ (PNN) crystal, a phase transition is typical that covers a wide temperature region [1]. Thanks to their unique electric performance, relaxor ferroelectric materials are applied in electronics [2]. To promote relaxors as materials for optical and optoelectronic applications, their photovoltaic properties shall be studied. Besides standard semiconductor research methods [3], there are techniques that use dynamic holography concepts [4], in particular, the non-steady-state photo-EMF method.

The non-steady-state photo-EMF effect is observed in the form of alternating current arising in a semiconductor illuminated by an oscillating interference pattern [5]. This current occurs due to periodic shifts of the conduction band (valence band) charge carrier grating against the space charge field grating concentrated on the trap centers. Current excitation involves electron generation into the conduction band and/or valence band, charge transfer as a result of drift and diffusion, trapping. This makes it possible to identify a set of photovoltaic properties of a material (type, value and relaxation time of conduction, charge carrier diffusion length, impurity center concentration) by measuring corresponding non-steady-state photo-EMF performance.

The previous study investigated the non-steady-state photo-EMF in PNN crystal in red light [6]. The purpose of this study is to investigate the effect on the wavelength corresponding to the light absorption edge of this material ($\lambda = 457$ nm). It is expected that the use of short-wavelength radiation will make it possible to achieve large signal amplitude which may be helpful for material applications.

2. Experimental setup

The experimental setup is shown in Figure 1. $\lambda = 457$ nm $P_{out} = 200$ mW single-frequency laser emission enters the interferometer where it is separated into two beams. The beams are directed to the test sample at a certain angle forming a fringe pattern with pre-defined intensity I_0, spatial frequency K and contrast $m = 0.39$. One of the beams is passed through an electrooptic modulator that performs sinusoidal light modulation with amplitude $\Delta = 0.51$ and frequency ω. As a result of such modulation, the fringe pattern becomes oscillating. Non-steady-state photo-EMF results in occurrence of alternating current on the load resistor $R_L = 100\,\text{k}\Omega \ldots 2.0\,\text{G}\Omega$, which then increases and is measured by a lock-in voltmeter. Current amplitude calculations include crystal capacitance and preamplifier input capacitance $C_{cr} + C_{in} = 4.4$ pF.

For direct measurement of the sample photoconductivity, a standard amplitude-modulated light technique is used [3]. In this case, constant voltage $U_{ext} = 600$ V is applied to the sample, the depth of sinusoidal light amplitude modulation is $m_{am} = 0.44$.

The study uses a $PbNi_{1/3}Nb_{2/3}O_3$ sample that was tested by us before at $\lambda = 660$ nm [6]. Dimensions of the sample are $1.2 \times 1.0 \times 0.25$ mm, surface treatment was not used. Electrodes were applied to the side surfaces (1.0×0.25 mm) using silver conductive paste.

3. Experimental results

For successful experiment with measurement of non-steady-state photo-EMF and for interpretation of results, it is of benefit to perform preliminary standard measurements of the photoconductivity response to the amplitude modulated

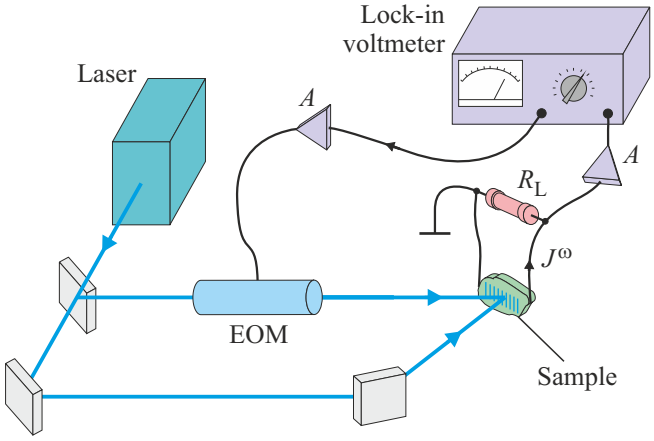

Figure 1. Experimental setup for non-steady-state photo-EMF investigation. *EOM* — electrooptic modulator, *A* — amplifier.

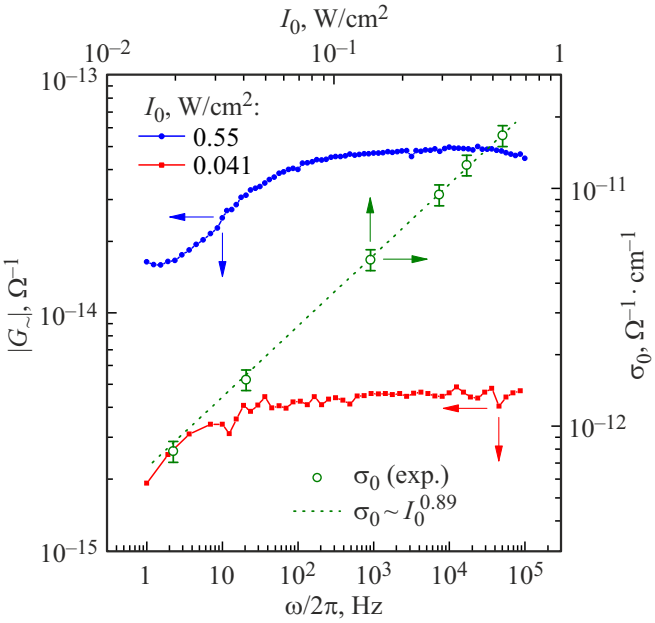

Figure 2. Frequency dependences of the photoconductivity response and dependence of specific photoconductivity on light intensity. PNN, $\lambda = 457$ nm.

light. Figure 2 shows frequency dependences of the response measured at two average light intensities. The absence of signal drop in the high frequency region is of interest. This means that the photoconductivity relaxation time shall be $\tau < 1\,\mu$s, and excitation of the non-steady-state photo-EMF in the same frequency range shall take place in quasi-steady-state conductivity conditions.

In theory, photoconductivity of a sample is determined by response values in low frequency region:

$$G_0 = R_0^{-1} = m_{am}^{-1} \lim_{\omega \to 0} |G_\sim(\omega)| \text{ [3].}$$

In the low frequency region, signal drop is observed that is probably caused by nonuniform illumination of the sample and nonuniform field near the blocking electrode, therefore we assume the response value on a frequency-independent section as a low-frequency limit ($\omega/2\pi = 10$ kHz). The calculated specific photoconductivity σ_0 depending on light intensity is shown in Figure 2. Calculations use reciprocal light absorptance $\alpha^{-1} = 0.082$ mm as an estimate of photoconductive layer thickness [6]. $\sigma_0(I_0)$ was found to be approximately linear $\sigma_0 \propto I_0^{0.89}$ indicating linearity of charge carrier generation and recombination.

Proceeding to non-steady-state photo-EMF experiments, it should be primarily noted that the expected increase in the signal amplitude excited by short-wavelength radiation ($\lambda = 457$ nm) compared with previous measurements in the red light region [6]. The signal-to-noise ratio reaches 50 dB making it possible to reliably detect signal in comparably wide measurement ranges of phase modulation frequency, intensity and spatial frequency. The non-steady-state photo-EMF signal phase corresponds to the hole-type photoconductivity of materials.

Curves of frequency vs. non-steady-state photo-EMF amplitude are shown in Figure 3. Signal generally demonstrates behavior typical for the effect of interest. The curves have a frequency-independent section and sections of growth and drop at low and high frequencies. In a low-frequency region, the photoconductivity and space charge gratings track displacements of the fringe pattern, a phase shift $\pi/2$ is maintained between the gratings, what is reflected in the smallness of the excited current. With frequency increase, the space charge grating becomes almost stationary, the amplitude of spatial shifts between the gratings increases, and the resulting current achieves its peak. With further increase in frequency, the photoconductivity grating also becomes stationary, the amplitude of relative spatial shifts of gratings becomes low, current decreases.

The listed frequency dependence sections are divided by co-called cutoff frequencies that are defined by $\sqrt{2}$ times signal amplitude drop from the peak value. In high-

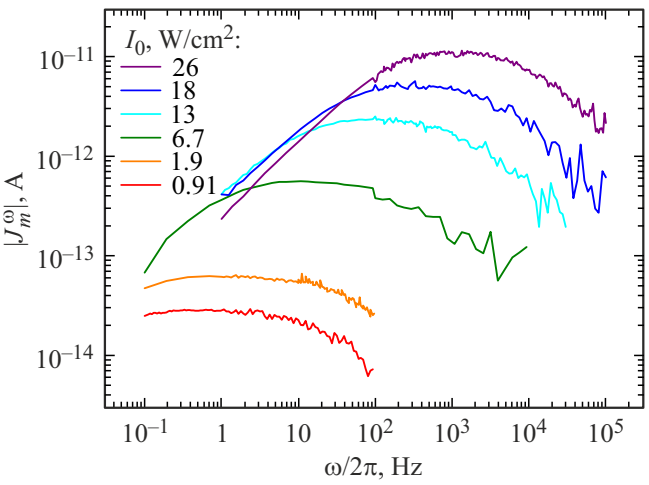

Figure 3. Frequency vs. non-steady-state photo-EMF amplitude. PNN, $\lambda = 457$ nm, $K = 0.31\,\mu$m^{-1}.

resistivity materials, the first cutoff frequency is defined by the Maxwell relaxation time $\tau_M = \epsilon\epsilon_0/\sigma_0$ [4]:

$$\omega_1 = [\tau_M(1 + K^2L_D^2)]^{-1}, \quad (1)$$

where L_D is the diffusion length of charge carriers, holes for the crystal of interest, $\epsilon = 1600$ is the dielectric permittivity of materials [1], ϵ_0 is the electric constant. The second cutoff frequency is defined by the photoconductivity relaxation time τ [5]:

$$\omega_2 = (1 + K^2L_D^2)/\tau. \quad (2)$$

This feature of the effect is used to determine photovoltaic properties of materials:

$$\sigma_0 = (1.1 \ldots 160) \cdot 10^{-9}\,\Omega^{-1}\text{cm}^{-1}\ (I_0 = 6.7 \ldots 26\,\text{W/cm}^2)$$

and

$$\tau = 16 \ldots 0.020\,\text{ms}\ (I_0 = 0.91 \ldots 26\,\text{W/cm}^2).$$

With light intensity growth, the maximum non-steady-state photo-EMF amplitude J_m^ω increases and is followed by the peak shift into the high frequency region. A signal amplitude increase itself is quite expected, and also for most photovoltaic phenomena. However, the dependence of maximum amplitude on intensity occurred to be approximately quadratic $|J_m^\omega| \propto I_0^2$ (Figure 4), which is non typical for the effect of interest: the dependence is usually described by an power function with an power varying from 0.5 to 1 for square and linear recombination of carriers, respectively [5].

The interference pattern spatial frequency is another experimental variable that defines the amplitude of the signal to be detected (Figure 5). The growth section on curve $|J_m^\omega(K)|$ is defined by the fact that the space charge grating amplitude involved in current excitation is proportional to the spatial frequency K [4]. If the spatial frequency becomes so high that the corresponding pattern period occurs to be much lower than the mean diffusion length, then „spreading" of the photoconductivity grating takes place, photoconductivity amplitude quickly decreases together with the resulting current. Such behavior is described by the following expression [5]:

$$J_m^\omega \propto \frac{K}{1 + K^2L_D^2}. \quad (3)$$

The best conditions for excitation of the non-steady-state photo-EMF occur at $K = L_D^{-1}$. Approximation of experimental dependences by these expressions makes it possible to assess the diffusion length: $L_D = 0.13 \ldots 0.17\,\mu\text{m}$ for $I_0 = 3.8 \ldots 26\,\text{W/cm}^2$.

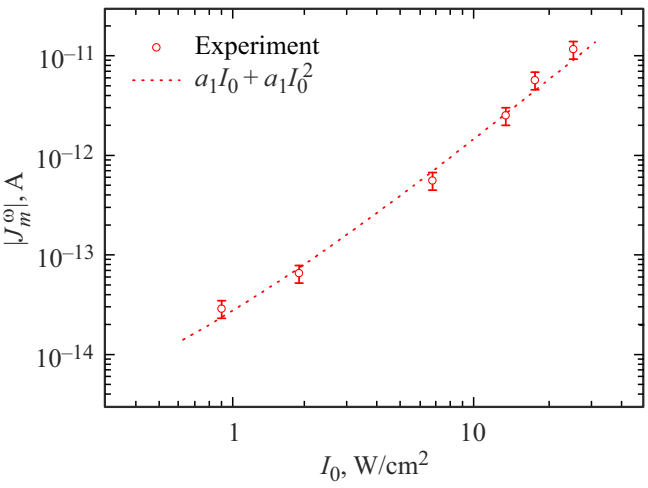

Figure 4. Maximum non-steady-state photo-EMF amplitude vs. mean light intensity. Polynomial approximation was used with coefficients $a_1 = 1.4 \cdot 10^{-14}\,\text{V}^{-1}\text{cm}^2$ and $a_2 = 1.3 \cdot 10^{-14}\,\text{A} \cdot \text{W}^{-2}\text{cm}^4$. PNN, $\lambda = 457\,\text{nm}$, $K = 0.31\,\mu\text{m}^{-1}$.

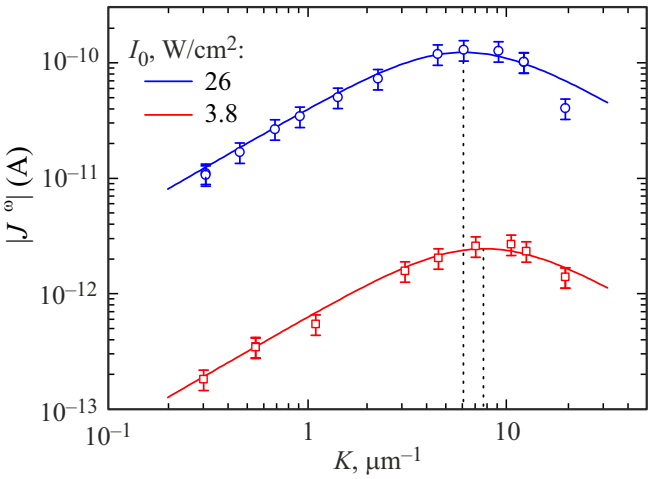

Figure 5. Maximum non-steady-state photo-EMF amplitude vs. interference pattern spatial frequency. Solid lines show approximation by expression (3). PNN, $\lambda = 457\,\text{nm}$.

4. Discussion

The non-steady-state photo-EMF signal excited in PNN crystal by blue light roughly follows the behavior observed earlier in some other materials [5]. However, there are features that need to be explained additionally. First, different behavior of $\sigma_0(I_0)$ and $|J_m^\omega(I_0)|$ that are approximately described by linear and quadratic functions, respectively, shall be noted. Second, there is the difference in specific photoconductivity estimates obtained by direct measurements and by analysis of frequency dependences of non-steady-state photo-EMF. Actually, extrapolation of directly measured $\sigma_0(I_0)$ to the intensity level used in the non-steady-state photo-EMF experiments gives $\sigma_0 = (0.16 \ldots 0.53) \cdot 10^{-9}\,\Omega^{-1}\text{cm}^{-1}$ $(I_0 = 6.7 \ldots 26\,\text{W/cm}^2)$. This is $7 \ldots 300$ times lower than the values derived from $|J_m^\omega(\omega)|$. Third, the increase in light intensity results in shift of $|J_m^\omega(K)|$ into the low spatial frequency region (Figure 5), then, as in the materials studied earlier, shift, if any, took place, but in the opposite direction.

All three listed features are probably associated with crystal heating by powerful laser beam light. As estimated, the sample temperature may reach $T = 600\,\mathrm{K}$ [6]. Since the temperature is included in expressions $E_D = (k_B T/e)K$ for the diffusion field and $L_D = [(k_B T/e)\mu\tau]^{1/2}$ or the diffusion length, then the specified variables become implicit light intensity functions (k_B is the Boltzmann constant, e is the elementary charge, μ is the charge carrier mobility). The diffusion field E_D defines the space charge field grating amplitude, which, in turn, defines the excited field amplitude. Position of the peak on the curve of signal amplitude vs. spatial frequency is associated with L_D. Thus, quadratic growth of the signal amplitude and shit of the peak on $|J_m^{\omega}(K)|$ with an increase in intensity are quite regular. Crystal heating also results in dielectric permittivity variation from $\epsilon = 1600$ at room temperature to $\epsilon = 350$ at $T = 600\,\mathrm{K}$ [1]. This means that the values for photoconductivity obtained from the frequency dependences of the non-steady-state photo-EMF amplitude shall be 4.5 times lower: $\sigma_0 = (0.24 \ldots 36) \cdot 10^{-9}\,\Omega^{-1}\mathrm{cm}^{-1}$ ($I_0 = 6.7 \ldots 26\,\mathrm{W/cm}^2$). After such correction, the photoconductivity values obtained by different methods do not have such high difference, at least, for not too high light intensities.

There is another feature which is currently hard to explain. Frequency dependences of the photoconductivity response have no pronounced declining section to frequencies about 100 kHz, then, like on the frequency dependences of the non-steady-state photo-EMF, the drop occurs beginning from frequencies about 10 Hz. Usually, the non-steady-state photo-EMF signal behavior in the high frequency region follows the features of the photoconductivity response, such correlation is not observed in the crystal of interest. Similar feature was observed earlier on the light wavelength $\lambda = 660\,\mathrm{nm}$ [6]. It could be assumed that the feature is attributed to the frequency dependence of the dielectric permittivity $\epsilon(\omega)$, however, numeric calculations show that the effect of this factor is limited by the low frequency region.

5. Conclusion

Excitation of non-steady-state photo-EMF in relaxor ferroelectric $PbNi_{1/3}Nb_{2/3}O_3$ by light corresponding to the absorption edge of this material. Signal properties measured in diffusion recording mode show both standard behavior and features associated with crystal heating by laser emission. Hole type of conductivity was established, specific photoconductivity and diffusion hole length were defined. Nontypical divergence of the frequency dependences of the photoconductivity response and non-steady-state photo-EMF was found and requires further experimental and theoretical investigation of the effect in this class of materials.

Conflict of interest

The authors declare that they have no conflict of interest.

References

[1] V.A. Bokov, I.E. Myl'nikova. FTT, **3**, (841), 1961 (1961). (in Russian).
[2] R.A. Cowley, S.N. Gvasaliya, S.G. Lushnikov, B. Roessli, G.M. Rotaru. Adv. Phys. **60**, *2*, 229 (2011).
[3] S.M. Ryvkin. Fotoelektricheskiye yavleniya v poluprovodnikakh. Fizmatgiz, M. (1963). 496 s. (in Russian).
[4] M.P. Petrov, S.I Stepanov, A.V. Khomenko. Fotorefraktivnyie krictally v kogerentnoy optike. Nauka, SPb. (1992). 320 p. (in Russian).
[5] I.A. Sokolov, M.A. Bryushinin. Optically induced space-charge gratings in wide-bandgap semiconductors: techniques and applications. Nova Science Publishers, Inc., N. Y. (2017). 229 p.
[6] M.A. Bryushinin, V.G. Zalesskii, A.D. Polushina, V.V. Kulikov, A.A. Petrov, S.G. Lushnikov, I.A. Sokolov. J. Opt. Soc. Am. B **38**, *7*, 2059 (2021).

Translated by 123